



QUIDEL

## MicroVue Pan-Specific C3 Reagent Kit

Expand the arsenal of Complement analysis in animals with the ability to detect depletion of C3.

Find out how this kit fills the gap of animal-specific Complement ELISA.



## Gap Junction Intercellular Communications Regulate NK Cell Activation and Modulate NK Cytotoxic Capacity

This information is current as of October 7, 2014.

Andrés Tittarelli, Ariadna Mendoza-Naranjo, Marcela Farías, Israel Guerrero, Fumitaka Ihara, Erik Wennerberg, Sebastian Riquelme, Alejandra Gleisner, Alexis Kalergis, Andreas Lundqvist, Mercedes N. López, Benedict J. Chambers and Flavio Salazar-Onfray

*J Immunol* 2014; 192:1313-1319; Prepublished online 27 December 2013;

doi: 10.4049/jimmunol.1301297

<http://www.jimmunol.org/content/192/3/1313>

**Supplementary Material** <http://www.jimmunol.org/content/suppl/2013/12/26/jimmunol.1301297.DCSupplemental.html>

**References** This article **cites 47 articles**, 24 of which you can access for free at: <http://www.jimmunol.org/content/192/3/1313.full#ref-list-1>

**Subscriptions** Information about subscribing to *The Journal of Immunology* is online at: <http://jimmunol.org/subscriptions>

**Permissions** Submit copyright permission requests at: <http://www.aai.org/ji/copyright.html>

**Email Alerts** Receive free email-alerts when new articles cite this article. Sign up at: <http://jimmunol.org/cgi/alerts/etoc>

*The Journal of Immunology* is published twice each month by The American Association of Immunologists, Inc., 9650 Rockville Pike, Bethesda, MD 20814-3994. Copyright © 2014 by The American Association of Immunologists, Inc. All rights reserved. Print ISSN: 0022-1767 Online ISSN: 1550-6606.



# Gap Junction Intercellular Communications Regulate NK Cell Activation and Modulate NK Cytotoxic Capacity

Andrés Tittarelli,<sup>\*,†,1</sup> Ariadna Mendoza-Naranjo,<sup>\*,†,1</sup> Marcela Farías,<sup>†</sup> Israel Guerrero,<sup>\*,†</sup> Fumitaka Ihara,<sup>\*</sup> Erik Wennerberg,<sup>§</sup> Sebastian Riquelme,<sup>¶</sup> Alejandra Gleisner,<sup>\*,†</sup> Alexis Kalergis,<sup>¶</sup> Andreas Lundqvist,<sup>§</sup> Mercedes N. López,<sup>\*,†,||</sup> Benedict J. Chambers,<sup>#</sup> and Flavio Salazar-Onfray<sup>\*,†</sup>

Gap junctions (GJs) mediate intercellular communication between adjacent cells. Previously, we showed that connexin 43 (Cx43), the main GJ protein in the immune system, mediates Ag transfer between human dendritic cells (DCs) and is recruited to the immunological synapse during T cell priming. This crosstalk contributed to T cell activation, intracellular Ca<sup>2+</sup> responses, and cytokine release. However, the role of GJs in NK cell activation by DCs and NK cell-mediated cytotoxicity against tumor cells remains unknown. In this study, we found polarization of Cx43 at the NK/DC and NK/tumor cell-contact sites, accompanied by the formation of functional GJs between NK/DCs and NK/tumor cells, respectively. Cx43-GJ-mediated intercellular communication (GJIC) between human NK and DCs was bidirectional. Blockage of Cx43-GJIC inhibited NK cell activation, though it affected neither the phenotype nor the function of DCs. Cx43 knockdown or inhibition using mimetic peptides greatly reduced CD69 and CD25 expression and IFN- $\gamma$  release by DC-stimulated NK cells. Moreover, blocking Cx43 strongly inhibited the NK cell-mediated tumor cell lysis associated with inhibition of granzyme B activity and Ca<sup>2+</sup> influx. Our data identify a novel and active role for Cx43-GJIC in human NK cell activation and antitumor effector functions that may be important for the design of new immune therapeutic strategies. *The Journal of Immunology*, 2014, 192: 1313–1319.

**G**ap junctions (GJs) are clusters of intercellular channels found in the plasma membrane that allow direct communication between adjacent cells (1). GJ channels are formed by two hexameric hemichannels (Hchs) or connexons, one provided by each of the two contacting cells. Connexons are formed by six polytopic *trans*-membrane protein subunits, termed connexins (Cxs), which provide permeability and regulatory

properties to the GJ channels (2). GJ-mediated intercellular communication (GJIC) is essential for the maintenance of cellular homeostasis and is involved in almost every aspect of cellular life (e.g., proliferation, cell differentiation, and cell death). GJs have a 1-kDa cutoff for the molecules that can be transferred from a donor to an acceptor cell. Thus, GJs allow exchange of small metabolites, ions, secondary messengers, and small peptides (2). Twenty-one different human Cx genes have been identified so far, each coding for a protein with the same topology (3). Whereas most Cx isoforms are expressed in a strictly tissue-specific manner, Cx43 is expressed ubiquitously (4).

Cell-cell contacts are one of the main forms of communication between cells of the immune system (5). Cx43 expression has been described in different types of immune system cells, including neutrophils, dendritic cells (DCs), macrophages, NK cells, T cells, and B cells (5, 6). Cxs and GJIC participate in key immunological processes, such as Ig secretion and cytokine production (7), transendothelial migration of leukocytes (8), peptide transfer and cross-presentation (9, 10), DC activation (11), regulatory T cell-mediated suppression through the transfer of cAMP (12), DC-mediated induction of IL-2 release, and proliferation of murine T cells (13). Recently, we showed that Cx43 accumulates at the immunological synapse (IS) during Ag-specific CD4<sup>+</sup> T cell priming, mediating bidirectional crosstalk between DCs and T cells. We demonstrated that Cx43-GJIC between DCs and T cells regulates Ca<sup>2+</sup> signals and T cell activation (14), pointing to a role for Cx43 as an important functional component for intercellular signaling in the immune system.

Immune surveillance by NK cells can lead to tumor rejection and control of tumor dissemination, in addition to protection against pathogens (15). DC–NK cell crosstalk is important for the activation of NK cells and can affect the magnitude and quality of the anti-tumor immune responses in vivo (16–19). It is known that the reciprocal activation of NK cells and DCs is a cell contact-dependent

<sup>\*</sup>Faculty of Medicine, Institute of Biomedical Sciences, University of Chile, 8380453 Santiago, Chile; <sup>†</sup>Millennium Institute on Immunology and Immunotherapy, University of Chile, 8380453 Santiago, Chile; <sup>‡</sup>University College London Cancer Institute, University College London, London WC1E 6DD, United Kingdom; <sup>§</sup>Department of Oncology and Pathology, Karolinska Institutet, 171 76 Stockholm, Sweden; <sup>¶</sup>Faculty of Biological Sciences, Millennium Institute on Immunology and Immunotherapy, Pontifical Catholic University of Chile, 8331010 Santiago, Chile; <sup>||</sup>Clinical Hospital Research Support Office, University of Chile, 8380453 Santiago, Chile; and <sup>#</sup>Department of Medicine, Center for Infectious Medicine, Huddinge University Hospital, Karolinska Institutet, 171 76 Stockholm, Sweden

<sup>1</sup>A.T. and A.M.-N. contributed equally to this work.

Received for publication May 15, 2013. Accepted for publication December 1, 2013.

This work was supported by grants from the National Fund for Scientific and Technological Development (1130320 to F.S.-O., 3070036 to A.M.-N., and 1130324 to M.N.L.), the Fund for the Promotion of Scientific and Technological Development (DO5110366 to F.S.-O. and M.N.L.), the Millennium Science Initiative from the Ministry for the Economy, Development and Tourism (P09/016-F) and the Swedish Cancer Foundation (to B.J.C.).

Address correspondence and reprint requests to Dr. Flavio Salazar-Onfray, Institute of Biomedical Sciences, Faculty of Medicine, University of Chile, Santiago 8380453, Chile. E-mail address: fsalazar@med.uchile.cl

The online version of this article contains supplemental material.

Abbreviations used in this article: AM, acetomethoxy; aNK, IL-2-activated NK cell; AS, antisense; Cx, connexin; Cx43, connexin 43; Cx43 s, connexin 43 sense; DC, dendritic cell;  $\beta$ -GA, 18- $\beta$ -glycyrrhetic acid; GJ, gap junction; GJIC, gap junction-mediated intercellular communication; GrB, granzyme B; Hch, hemichannel; iDC, immature DC; IS, immunological synapse; mDC, mature DC; MFI, mean fluorescence intensity; MIP-1 $\beta$ , macrophage inflammatory protein-1 $\beta$ ; ODN, oligodeoxynucleotide; rNK, resting NK cell.

Copyright © 2014 by The American Association of Immunologists, Inc. 0022-1767/14/\$16.00

process and mediated through the formation of a functional IS (18). Moreover, NK-mediated cytotoxicity of target cells largely relies on the formation of functional IS (20). Once an IS is formed, NK cells can induce apoptosis in the target cells by releasing their cytotoxic granules, including granzyme B (GrB) (21). Importantly,  $\text{Ca}^{2+}$  influx in target cells is required for the effective internalization of perforin and GrB and for immune-mediated death by apoptosis (21). In the current study, we describe for the first time, to our knowledge, that Cx43, the main GJ protein of the immune system (4), accumulates at the contact zone of NK cells and DCs or at the interface between NK cells and target cells, facilitating DC-mediated NK cell activation and cytotoxic activity against tumor cells.

## Materials and Methods

### *Cell lines, generation of DCs, and NK cell purification*

This study was approved by the Bioethical Committee of Human Research, Faculty of Medicine, University of Chile. Mel1 and Mel3 are human melanoma cell lines established from metastatic lymph nodes biopsies at the Institute of Biomedical Sciences, University of Chile (22). The myelogenous leukemia cell line K562 was purchased from American Type Culture Collection. The cells were grown at 37°C in an atmosphere with 5%  $\text{CO}_2$  in RPMI 1640 culture medium (Invitrogen) supplemented with 10% FBS, penicillin (100 U/L), streptomycin (100 mg/ml), and 1 mM L-glutamine (all from Invitrogen).

Leukocytes from healthy donors were isolated by density gradient using Ficoll-Hypaque (Axis-Shield). Human DCs were obtained as described (10). At day 6, DCs were stimulated overnight with 100  $\mu\text{g}/\text{ml}$  melanoma cell lysate named TRIMEL, which was obtained as previously described (23), and with 2 ng/ml recombinant human TNF- $\alpha$  (U.S. Biological; TRIMEL-matured DCs [mDCs]). Nonstimulated DCs correspond to the immature DCs (iDCs).

Resting (r)NK cells were purified by negative selection from PBMCs using the NK Cell Isolation Kit (Miltenyi Biotec) according to the manufacturer's instructions. Purity of the isolated  $\text{CD}3^- \text{CD}56^+$  NK cells was >90% according to routinely performed flow cytometry analysis. NK cells were activated overnight (IL-2-activated NK cells [aNK cells]) with 500 U/ml recombinant human IL-2 (ProSpec-Tany TechnoGene).

### *Inhibition of Cx43 channels and GJs*

DCs, NK cells, and tumor cells were pretreated as follows: 4 h with 40  $\mu\text{M}$  Cx43 antisense (Cx43-AS) human oligodeoxynucleotide (ODN) (sequence: 5'-gTA ATg Cgg CAA gAA gAA TTg TTT CTg TC-3') or 40  $\mu\text{M}$  Cx43 sense (Cx43 s) ODN (24); and 30 min with 300  $\mu\text{M}$  1848-mimetic peptide (sequence: CNTQQPGCENVCY; extracellular loop 1; >98% purity), 300  $\mu\text{M}$  gap20 control peptide (sequence: EIKKFKYGIEEHC; cytoplasmic loop; >98% purity; both from China Peptides), or 50  $\mu\text{M}$  18- $\beta$ -glycyrrhetic acid ( $\beta$ -GA; Sigma-Aldrich). For incubations lasting >4 h, the ODNs and mimetic peptides were added every 4 h.

### *Abs and flow cytometry analysis*

Flow cytometry experiments were performed as previously described (10). To detect Cx43, a rabbit polyclonal anti-human Cx43 Ab, directed to the C-terminal domain (C6219; Sigma-Aldrich), plus a secondary donkey anti-rabbit FITC-conjugated Ab (Poly4064; BioLegend) were used. The following mAbs were used for cell staining: anti-CD11c (clone 3.9), anti-CD3 (clone OKT3), anti-CD56 (clone CMSSB), anti-CD69 (clone FN50), anti-CD25 (clone BC96), anti-CD107a (clone H4A3; all from eBioscience), anti-macrophage inflammatory protein-1 $\beta$  (MIP-1 $\beta$ ; D21-1351; BD Biosciences), and LFA-1 mAb24 (25) (ab13219; Abcam). To simultaneously evaluate active LFA-1, CD107a surface expression, and intracellular MIP-1 $\beta$  expression on PBMCs cocultured or not with K562 cells, we performed a multiparameter flow cytometry analysis as previously described (26). Samples were acquired on an FACSCalibur (BD Biosciences) or a CyAN ADP LX 9-color flow cytometer (DakoCytomation) and analyzed using the software Cyflogic (version 1.2.1; CyFlo) or FlowJo (version 8.8.6; Tree Star).

### *Immune fluorescence staining, confocal microscopy, and quantitative image analysis*

Purified rNK or aNK cells were cocultured with autologous iDCs or TRIMEL-stimulated mDCs for 30 min or with K562, Mel1, or Mel3 tumor cells prestained with the fluorescent dye CM-Dil (15  $\mu\text{g}/\text{ml}$ ) according to the manufacturer's indications (Invitrogen) at a ratio of 3:1 for 0, 10, 30, and 60 min. The cell conjugates were gently washed with PBS twice and

fixed with 4% paraformaldehyde for 30 min. After gentle washing with PBS, the cells were incubated in ammonium chloride (50  $\mu\text{M}$ ) for 10 min. Then the cells were permeabilized for 10 min (0.5% Triton X-100 and 0.5% FBS) and blocked with 0.5% BSA. We allowed the conjugates to adhere to poly-L-lysine-coated slides (Sigma-Aldrich), and the cell mixture was incubated with the PE-conjugated anti-CD11c (clone 3.9; eBioscience), APC-conjugated anti-CD56 (clone CMSSB; eBioscience) mAbs, and anti-Cx43 polyclonal Abs (C6219; Sigma-Aldrich) overnight at 4°C. Cx43 expression was visualized by using the secondary donkey anti-rabbit FITC-conjugated Ab (Poly4064; BioLegend); additionally, cells were also stained with 5  $\mu\text{g}/\text{ml}$  Hoechst 33342 (Invitrogen) and mounted using DAKO fluorescence mounting medium (DakoCytomation). Cells were analyzed by confocal microscopy (LSM 510; 363 numerical aperture 1.4 oil immersion objective; Carl Zeiss).

The recruitment of Cx43 to the cell-contact site was quantified using the ImageJ NIH software and quantified as the ratio of the Cx43 mean fluorescence intensity (MFI) in the cell-contact site versus the Cx43 MFI in the same area but in the opposite side of the cell-contact site. Between 40 and 60 NK cell-DCs or NK cell-target cell conjugates were analyzed on ~30 fields in at least three experiments. Two independent investigators evaluated the data. The fluorescence emission intensity was displayed on a pseudocolor scale (16 colors) using the Image J software (National Institutes of Health).

### *Calcein-acetomethoxy and GJIC detection*

GJIC was measured using calcein transfer assay as previously described (27). DCs, isolated NK cells, K562, or melanoma cells were loaded with calcein-acetomethoxy (AM) (1  $\mu\text{M}$ ; Sigma-Aldrich) or the plasma membrane red marker CM-Dil (15  $\mu\text{g}/\text{ml}$ ; Invitrogen) for 30 min at 37°C according to the manufacturer's instructions. The membrane-permeable calcein-AM is hydrolyzed by intracellular nonspecific esterase, and the resulting green fluorescent hydrophilic calcein is then trapped inside the cells. GJs are permeable to calcein but not to CM-Dil. Dil-stained cells were cocultured with calcein-stained cells for different times and at different ratios in the presence or absence of the Cx43 inhibitors. After cocultures, the cells were collected and analyzed by flow cytometry.

### *IFN- $\gamma$ ELISPOT assay*

Isolated rNK cells were cocultured with autologous TRIMEL-stimulated mDCs for 12 h at a ratio 10:1 in the presence or absence of 300  $\mu\text{M}$  Cx43-mimetic peptides 1848 and gap20. IFN- $\gamma$  release was tested by ELISPOT assay according to the manufacturer's instructions (Mabtech).

### *[ $^{51}\text{Cr}$ ] release assay*

The cytotoxic activity of isolated aNK cells was measured by conventional 4-h [ $^{51}\text{Cr}$ ] (PerkinElmer) release assays using triplicate cultures in round-bottom 96-well plates in the presence or absence of the different Cx43 inhibitors. E:T cell ratios were as indicated, on 5000 target cells/well. Specific lysis was calculated according to the formula: percent specific lysis = [(experimental release - spontaneous release)/(maximum release - spontaneous release)]  $\times$  100.

### *Measurement of GrB activity*

Isolated aNK and K562 cells were preincubated or not with 300  $\mu\text{M}$  Cx43-mimetic peptide 1848 or control peptide gap20. GrB activity was measured by GranToxiLux kit (OncoImmunit) according to the manufacturer's protocol. Labeled K562 cells were cocultured with NK cells for 1 h at a 1:3 ratio, in the presence of a permeable fluorogenic substrate for GrB. GrB activity was evaluated in K562 cells (TFL4 $^+$ CD56 $^-$ ) by flow cytometry.

### *Measurement of intracellular calcium*

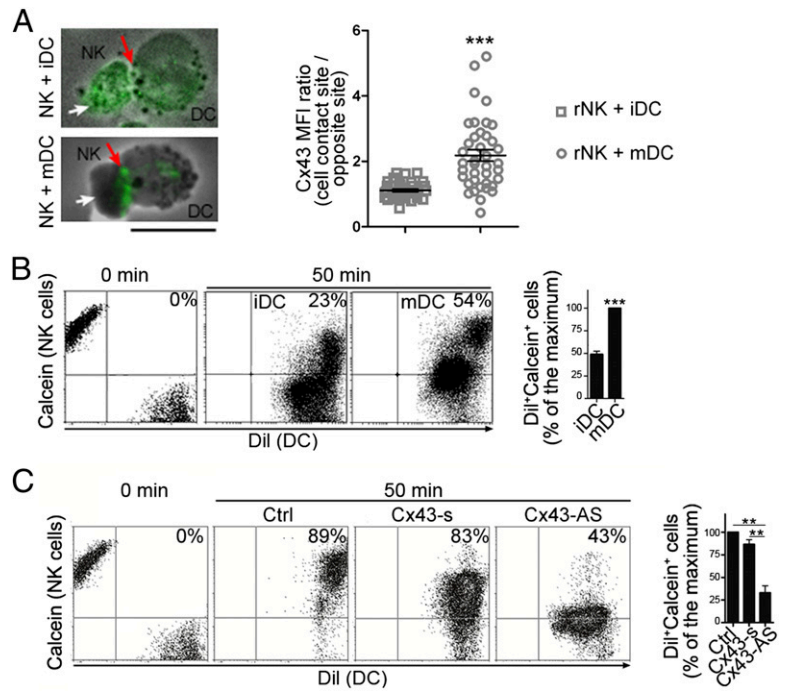
K562 or Mel3 cells were loaded with 5  $\mu\text{M}$  Fluo4-AM (Invitrogen) according to the manufacturer's protocol. Intracellular  $\text{Ca}^{2+}$  levels were measured by flow cytometry in target cells cocultured with aNK cells at a 1:3 ratio at different time points as previously described (28). Cells were incubated with the Cx43-mimetic peptide 1848 or control peptide gap20 before and during the cocultures. Fluo4-AM fluorescence ratio ( $F_1/F_0$ ) intensity was plotted as a function of time.

## Results

### *NK cells and DCs communicate through functional Cx43-mediated GJs*

Previously, we demonstrated that Cx43 accumulates in the IS during DC-mediated priming of  $\text{CD}4^+$  T cells, promoting lymphocyte

**FIGURE 1.** NK cells and DCs communicate through functional Cx43-mediated GJs. **(A)** The distribution of Cx43 was analyzed using a polyclonal anti-Cx43 Ab plus a secondary FITC-conjugated mAb by confocal microscopy 30 min after coincubation of autologous iDC-rNK cells or mDC-rNK cells. The cell-contact site is indicated with a red arrow, and the opposite site is indicated with a white arrow. Images are representative of three independent experiments. The right panel shows the Cx43 accumulation at the cell-contact site, which was measured as the ratio of the Cx43 MFI at the cell-contact site versus the opposite site and was evaluated in the different cocultures. Values are reported as mean  $\pm$  SD of three independent experiments. Scale bar, 5  $\mu$ m. **(B)** Isolated aNK cells were preloaded with calcein-AM and cocultured for 50 min with autologous iDCs or TRIMEL-stimulated mDCs preloaded with Dil. The calcein transfer from the NK cells to the DCs was assessed by flow cytometry. The numbers in the dot plots represent percentage of Dil<sup>+</sup>Calcein<sup>+</sup> cells. The bar graph shows Dil<sup>+</sup>Calcein<sup>+</sup> cells as a percentage of the maximum (mDCs);  $n = 3$  independent experiments. **(C)** Isolated aNK cells were preloaded with calcein and cocultured for 50 min with autologous TRIMEL-stimulated mDCs preloaded with Dil. Cells were pretreated for 4 h with the Cx43-AS or the Cx43 s. Percentages of Dil<sup>+</sup>Calcein<sup>+</sup> cells are indicated. The bar graph shows Dil<sup>+</sup>Calcein<sup>+</sup> cells (as a percentage of the maximum [control (Ctrl)]);  $n = 3$  independent experiments.  $**p < 0.01$ ,  $***p < 0.001$ .



activation through the formation of functional GJs and increased intracellular Ca<sup>2+</sup> signaling in T cells (14). Given that the reciprocal activation of DCs and NK cells is a cell contact-dependent process and shares some mechanisms with the DC-mediated T cell priming such as the formation of a functional IS (18), we aimed to examine whether Cx43-GJ channels may be involved in DC-NK intercellular communication. In line with previously published data (6), positive Cx43 expression was observed in NK cells, and the expression levels were similar to rNKs and aNKs, respectively (Supplemental Fig. 1A). Cx43 levels were increased in mDCs compared with nonstimulated iDCs (Supplemental Fig. 1B), as previously reported (10, 11). The Cx43 cellular distribution was then investigated by confocal microscopy in conjugates of iDCs or mDCs with autologous rNK cells. Cx43 was found to preferentially accumulate in the interface between mDCs and the rNK cells, but was homogeneously distributed when rNK cells were incubated with iDCs (Fig. 1A).

GJ-mediated bidirectional communication between cells of the immune system has been previously described (7, 14). The establishment of bidirectional GJIC between DCs and NK cells was monitored using a calcein transfer assay. iDCs or mDCs were loaded with the GJ nondiffusible dye CM-Dil (Fig. 1B, 1C) or the GJ diffusible dye calcein-AM (Supplemental Fig. 1C) and cocultured for 50 min with autologous rNK cells loaded with calcein-AM or CM-Dil, respectively. There was an ~2-fold increase in calcein-AM dye transfer from mDCs to rNK cells compared with the transfer from iDCs (Fig. 1B). This result is consistent with the augmented Cx43 expression levels in mDCs (Supplemental Fig. 1B). Inhibition of Cx43 by a Cx43-AS ODN that targets Cx43 expression in NK cells and DCs (Supplemental Fig. 2) blocked the calcein-AM transfer from rNK cells to mDCs, confirming that Cx43 is required for functional GJIC between these immune cells (Fig. 1C). Similar results were obtained using  $\beta$ -GA, which inhibits GJ formation by dephosphorylation of Cxs (29) (Supplemental Fig. 1C). These results demonstrate a role for Cx43 in mediating bidirectional intercellular communication between NK cells and mDCs.

*Cx43 channels are required for DC-mediated NK cell activation*

Human NK cells are activated by mature monocyte-derived DCs (16, 30). To investigate whether Cx43-mediated intercellular communication is involved in mDC-mediated activation of autologous rNK cells, CD69 and CD25 surface expression was evaluated in NK cells cocultured with mDCs in the presence of the Cx43-mimetic peptide 1848, which blocks docking between adjacent Cx43 Hchs (14). Induction of CD69 and CD25 on NK cells was strongly inhibited after treatment with the 1848 Cx43-mimetic peptide (Fig. 2A, 2B). In contrast, incubation with the

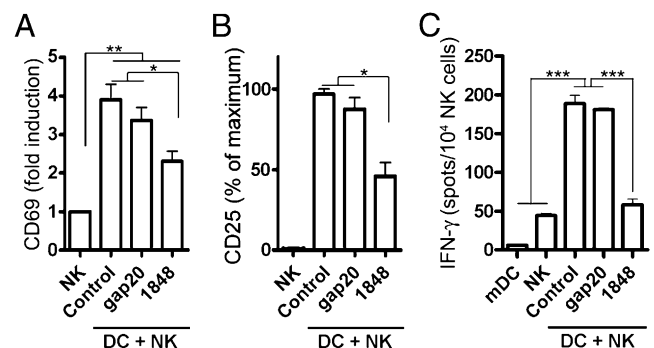


**FIGURE 2.** Cx43 GJIC is required for DC-mediated NK cell activation. **(A and B)** Autologous mDCs and rNK cells were cocultured for 20 h with NK cells (in a 3:1 ratio of NK/DCs), in the presence or absence of the Cx43-mimetic peptide 1848 or the control peptide gap20. CD69 (A) and CD25 (B) surface expression was determined in the CD3<sup>-</sup>CD56<sup>+</sup> NK cell population by flow cytometry and plotted as fold induction, relative to the level of NK cells alone (A) or as percentage of the maximum expression (B). Data correspond to the mean  $\pm$  SD from three independent experiments. **(C)** Autologous TRIMEL-stimulated mDCs and rNK cells were cocultured for 12 h at a 10:1 ratio of NK cells/DCs in the presence or absence of the Cx43-mimetic peptide 1848 or the control peptide gap20. The secretion of IFN- $\gamma$  was assessed by ELISPOT. Results correspond to the mean  $\pm$  SD from three independent experiments.  $*p < 0.05$ ,  $**p < 0.01$ ,  $***p < 0.001$ .

control gap20 peptide did not affect CD69 or CD25 expression levels (Fig. 2A, 2B). Similarly, treatment of mDCs and NK cells with the Cx43-mimetic peptide 1848 severely impaired IFN- $\gamma$  secretion by NK cells (Fig. 2C). Although Cx43-GJIC between NK cells and DCs was bidirectional (Fig. 1, Supplemental Fig. 1), Cx43-mediated interaction between NK and DCs did not affect surface expression of different markers on DCs, including MHC class I and II, the maturation molecules CD83 and CD86, and NK-

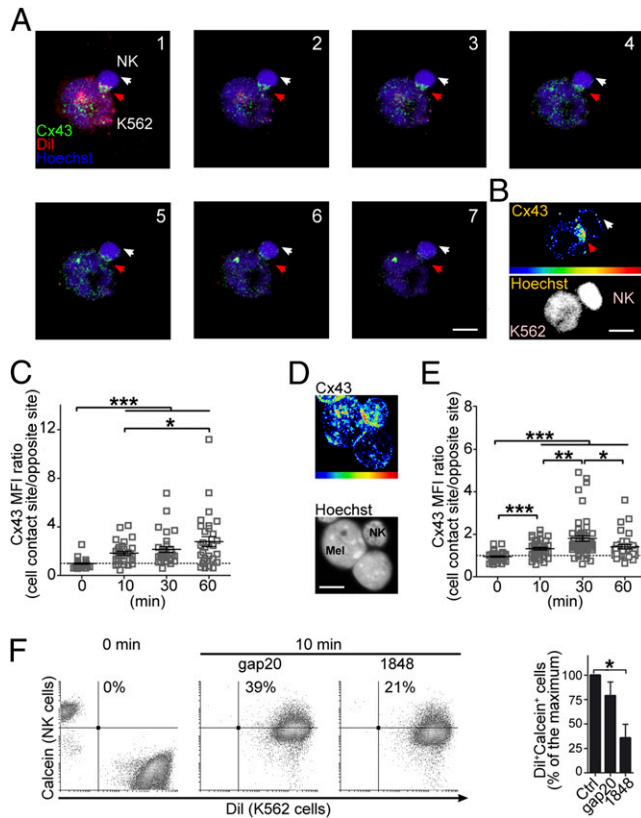


**FIGURE 3.** Cx43 accumulates at the site of cell contact during the killing of NK cell-sensitive tumor cell lines. **(A)** Representative images of Cx43 distribution (green) 30 min after coculture of aNK and K562 cells prestained with Dil (red). A series of images (1–7) obtained by serial optical sections of the same cells at 1- $\mu$ m thickness along the z-axis are shown. Blue: Hoechst nuclear staining. The cell-contact site is indicated with a red arrowhead, whereas the opposite site is indicated with a white arrowhead. **(B)** Cx43 accumulation at the cell-contact site, depicted in pseudocolor, in aNK cell and K562 conjugates. *Bottom panel* shows Hoechst nuclear staining. Scale bars in (A) and (B), 5  $\mu$ m. **(C)** Cx43 accumulation at the cell-contact site was measured as the ratio of the Cx43 MFI at the cell-contact site versus at the opposite site and was evaluated at different times of coculture between aNK cells with K562 cells. Values are reported as mean  $\pm$  SD of three independent experiments. **(D)** A pseudocolor image shows Cx43 accumulation at the cell-contact site formed between aNK and Mel3 cells 60 min after of coculture. The black and white picture depicts nuclear Hoechst staining. Scale bar, 5  $\mu$ m. **(E)** Cx43 accumulation at the cell-contact site formed between aNK cells and Mel3 cells was measured as described in (C). Values are reported as the mean  $\pm$  SD of three independent experiments. **(F)** aNK cells and K562 cells communicate through functional Cx43 channels. Calcein transfer assays were carried out after 10 min of coculture of isolated aNK cells (labeled with calcein) and K562 cells (labeled with Dil) pretreated or not with the Cx43-mimetic peptide 1848 or gap20. The percentage of Dil<sup>+</sup>Calcein<sup>+</sup> cells is indicated. The bar graph shows the Dil<sup>+</sup>Calcein<sup>+</sup> cells as percentage of the maximum (cells without peptides [control (Ctrl)]) and corresponds to the results from three independent experiments. These data are comparable with results obtained with Mel3 as target cells. \* $p$  < 0.05, \*\* $p$  < 0.01, \*\*\* $p$  < 0.001.

associated MICA and MICB molecules known to act as key ligands for NKG2D and promote NK cell-mediated recognition and cytotoxicity (31). Moreover, Cx43 blocking or silencing affected neither the expression of these markers (Supplemental Fig. 3A, 3B) nor the NK-induced TNF- $\alpha$  or IL-12 release by iDCs or activated DCs (Supplemental Fig. 3C, 3D). Finally, Cx43-mimetic peptides neither affect NK cell viability nor DC maturation state (Supplemental Fig. 2).

*Cx43 accumulates at site of contact between NK cells and tumor cells, which contributes to NK cell-mediated cytotoxic activity against tumor cells*

Tumor elimination by NK cells largely relies on the formation of an IS between the cytotoxic cells and their targets (20). To determine whether NK cells and tumor cells can communicate through Cx43 channels, aNK cells were cocultured with K562 cells, an NK-sensitive myelogenous leukemia cell line, and the distribution of Cx43 was analyzed by confocal microscopy. Cx43 was found to accumulate at the interface between the NK cells and K562 cells (Fig. 3A, 3B). This accumulation was observed as soon as 10 min after coculture and significantly increased following 60 min of coculture (Fig. 3C). A similar phenotype of accumulated Cx43 at the site of contact with NK cells was observed in two different human melanoma cell lines, Mel1 and Mel3 (Fig. 3D, 3E and data not shown). Moreover, NK cells and target cells (K562 and Mel3 cells) formed bidirectional coupling through Cx43 channels, which was effectively reduced by blocking Cx43-GJIC (Fig. 3F, Supplemental Fig. 4A).

Both Cx43 Hchs as well Cx43-GJs play an important role in the intercellular communication of death signals (32). However, an

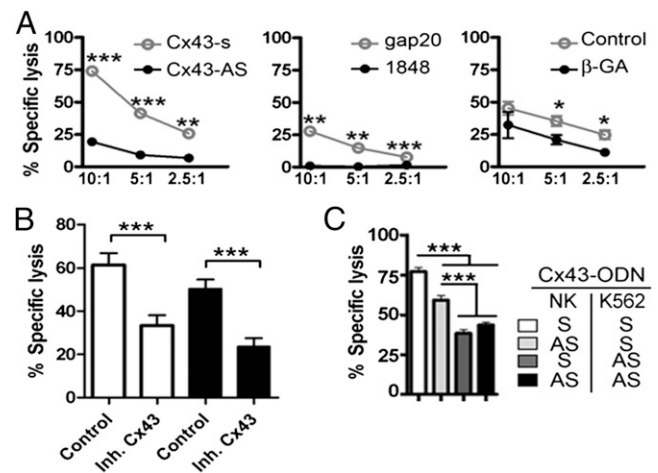


**FIGURE 4.** Cx43-mediated intercellular communication contributes to NK cell cytotoxic activity against tumor cells. **(A)** IL-2-activated aNK cells were cocultured with K562 cells at different E:T ratios and preincubated with Cx43 and GJ inhibitors or their respective controls. Cytotoxicity was assessed by conventional [<sup>51</sup>Cr] release assays. The results are plotted as a percentage of specific lysis and are representative of at least three independent experiments and comparable with those obtained in the melanoma cell lines (Mel1 and Mel3) as target cells. **(B)** Combined results from nine independent [<sup>51</sup>Cr] release assays using aNK cells and different tumor cells are shown (E:T ratio, 10:1). White bars indicate target/K562 cells; black bars indicate target/Mel3 cells. Cytotoxic assays were performed using different Cx43 and GJ inhibitors [(Inh.); Cx43-mimetic peptide 1848, Cx43-AS, and  $\beta$ -GA] or their respective controls. **(C)** aNKs or K562 cells were pretreated with the Cx43-AS or Cx43 s (S), and cytotoxic activity was determined by [<sup>51</sup>Cr] release assays at an E:T ratio of 10:1. The graph shows the percentage of specific lysis represented as the mean  $\pm$  SD of three independent experiments. \* $p$  < 0.05, \*\* $p$  < 0.01, \*\*\* $p$  < 0.001.

important and unexplored aspect of these Cx43 channels is whether they play a role in NK cell–mediated cytotoxicity. Using conventional [ $^{51}\text{Cr}$ ] release assays, we observed that NK cell cytotoxic activity against tumor cells was significantly reduced following treatment with Cx43-AS, the Cx43-mimetic peptide 1848, or the GJ inhibitor  $\beta$ -GA (Fig. 4A, 4B). Overall, inhibition of GJs and specific inhibition of Cx43 reduced NK cell–mediated tumor lysis by  $\sim 50\%$  (Fig. 4B).

In contrast to Hch-based signaling, communication via GJ channels requires expression of Cx proteins in both donor and recipient cells. To further analyze how Cx43 regulates NK cell cytotoxic activity, Cx43 expression was silenced using Cx43-AS only in NK cells, only in K562 cells, or in both. Knockdown of Cx43 in NK cells resulted in a significant reduction of NK cytotoxic activity (Fig. 4C). However, cytotoxic activity was dramatically impaired when Cx43 expression was targeted in K562 cells only, or in both NK and K562 cells (Fig. 4C), probably due to the fact that the Cx43 knockdown was more effective in K562 cells than in NK cells (Supplemental Fig. 2B). Taken together, these findings reveal that Cx43 accumulation at the site of interaction between NK cells and tumor cells appears to regulate NK cell–mediated cytotoxic activity against tumor cells.

*Cx43-mediated intercellular communication contributes to an efficient GrB activity and calcium influx in target cells during the NK cell attack*

GrB is a proapoptotic serine protease that plays a crucial role in NK cell–mediated cytotoxicity (21, 33, 34). Following the recognition of target cells and activation, NK cells release mature GrB specifically in the IS, from where it enters target cells in cooperation with perforin, rapidly inducing their death. In order to assess the

contribution of GJs to this process, GrB activity was examined in control (treated with gap20 peptide) or Cx43-deficient (treated with the Cx43 mimetic peptide) K562 cells. Significantly lower intracellular GrB activity was detected in K562 cells cocultured with NK cells following inhibition of Cx43 (Fig. 5A). This finding suggests that Cx43 channels may somehow contribute to the efficient GrB activity in the target cells during NK cell–mediated cytotoxicity. The engagement of activating receptors at the lytic IS site during target cell recognition induces the so-called inside-out signals that prompt an extracellular conformational change in LFA-1. This integrin switch from a closed to an open, extended conformation facilitates ligand binding and target cell adhesion (35) and in turn can support LFA-1–dependent signals for cytotoxic granule polarization, maturation, and NK-mediated cytotoxicity (36). Inhibition of Cx43-mediated intercellular communication during tumor recognition by NK cells did not affect LFA-1 active conformational change in NK cells (Fig. 5B). CD107a (LAMP-1)-deficient cells have reduced levels of perforin in lytic granules and disturbed motility of the lytic granules, which leads to the inability to deliver apoptosis-inducing GrB to target cells and to the inhibition of NK cell cytotoxicity (36, 37). We evaluated CD107a expression on the surface of NK cells; however, no difference in CD107a levels were observed upon blockade of Cx43-GJs in NK cells and K562 cells (Fig. 5C). This suggests that the reduced cytotoxicity observed following GJ blockage was not due to reduced degranulation by NK cells. Furthermore, inhibition of Cx43-mediated intercellular communication during tumor recognition by NK cells did not affect CD69 or MIP-1 $\beta$  expression levels in NK cells (Supplemental Fig. 4B, 4C).

During NK cell–mediated cytotoxicity, a transient  $\text{Ca}^{2+}$  influx is induced in the target cells, which is necessary for the apoptosis

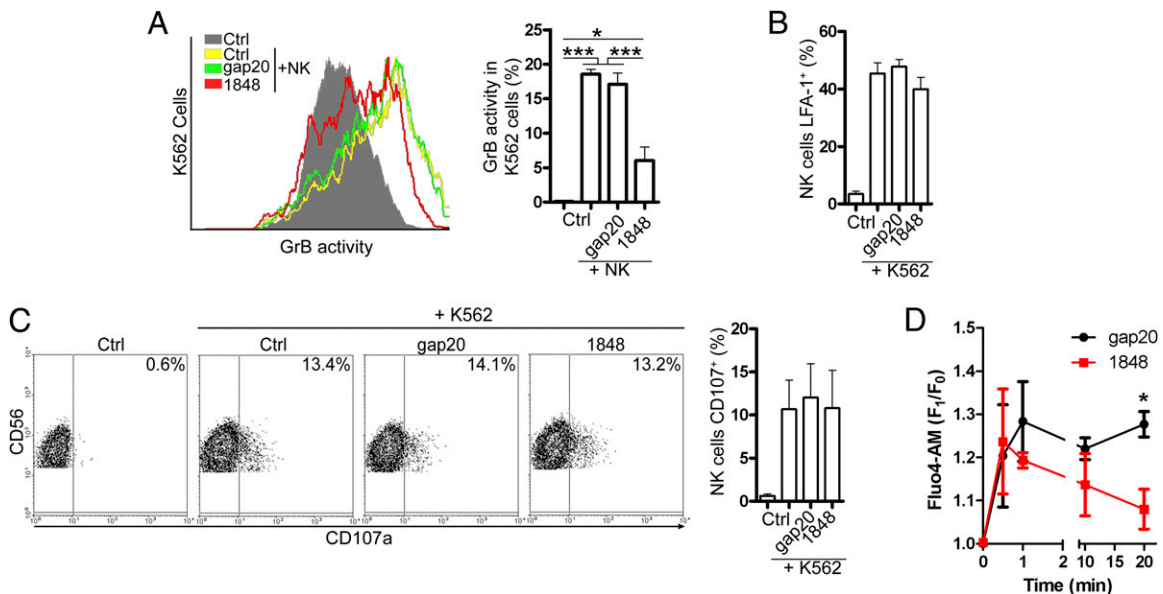


**FIGURE 5.** Cx43-mediated GJIC contributes to efficient GrB activity and calcium influx in target cells during the NK cell–mediated cytotoxicity of tumor cells. **(A)** aNK and K562 cells were pretreated or not with the Cx43-mimetic peptide 1848 or the control peptide gap20. K562 cells were labeled with TFL4 and cocultured with the aNK cells for 1 h at an E:T ratio of 3:1 in the presence of a permeable fluorogenic substrate for GrB. GrB activity was evaluated in K562 cells (TFL4<sup>+</sup>CD56<sup>+</sup>) by flow cytometry. Histograms depict one of three representative experiments. The graph represents the average percentage of GS<sup>+</sup> K562 cells  $\pm$  SD of three independent experiments. **(B)** PBMCs preincubated or not with the Cx43-mimetic peptide 1848 or the control peptide gap20 were cocultured or not for 2 h with K562 cells at a 1:1 ratio. Active conformation LFA-1 expression was determined by multiparameter flow cytometry on CD3<sup>+</sup>CD56<sup>+</sup> NK cells. The bars represent the average values of the MFI  $\pm$  SD of three independent experiments. **(C)** PBMCs preincubated or not with the Cx43-mimetic peptide 1848 or the control peptide gap20 were cocultured or not with K562 cells at a 1:1 ratio. CD107a surface expression was determined on CD3<sup>+</sup>CD56<sup>+</sup> NK cells. Bars represent the average MFI  $\pm$  SD of three independent experiments. **(D)** Intracellular  $\text{Ca}^{2+}$  levels were measured by flow cytometry in Fluo4-AM preloaded target cells incubated for different time points with aNK cells at an E:T ratio of 3:1. Cells were treated with the Cx43-mimetic peptide 1848 or the control peptide gap20. Fluo4-AM fluorescence ratio (F<sub>1</sub>/F<sub>0</sub>) intensity was plotted as a function of time. The data are represented as the results from three different experiments using K562 as target cells. \* $p < 0.05$ , \*\*\* $p < 0.001$ . Ctrl, Control.

triggered by the endocytosed GrB (21, 37, 38). It is known that Cx43 regulates  $\text{Ca}^{2+}$  influx in various cell types (39), and we have previously reported that Cx43 regulates  $\text{Ca}^{2+}$  signaling at the IS in T cells (14). Calcium signaling impacts on the granule trafficking pathways through the regulation of  $\text{Ca}^{2+}$ -responsive proteins to facilitate the rapid movement and fusion of secretory granules with the plasma membrane and is essential for degranulation events in NK cells (40). Additionally, Cx43 channels can mediate the intercellular transfer of death signals (32), and previous evidence suggests that  $\text{Ca}^{2+}$  could be a major cell death messenger passing through Cx43 channels (41). In order to evaluate whether GJ contribution to GrB cytotoxicity could be facilitated by Cx43-mediated regulation of  $\text{Ca}^{2+}$  signaling, intracellular  $\text{Ca}^{2+}$  levels were evaluated in Fluo4-AM preloaded target cells cocultured with control and Cx43-deficient NK cells. Inhibition of Cx43 by the 1848 mimetic peptide significantly impaired intracellular  $\text{Ca}^{2+}$  signaling 20 min after coculture with NK cells (Fig. 5D). These data indicate that Cx43 intercellular communication contributes to the efficient GrB activity and increase in  $\text{Ca}^{2+}$  influx observed in the target cells in contact with NK cells, which consequently potentiate NK cell-mediated cytotoxicity against tumor cells.

## Discussion

The essential role of Cxs and GJs regulating key immunological processes has become increasingly clear in recent years (4–14). Although Cx43 expression in NK cells was first described over a decade ago (6), the role of Cx43 in NK cell function and activation remains largely unknown. In the current study, we have found that NK cells can form bidirectional and functional GJIC with DCs and tumor cells via Cx43.

Cx43 expression and GJ formation in DCs is a means by which DCs can communicate with themselves and with T cells (10, 14). More recently, DCs have also been shown to activate NK cells (16–19, 30). NK cell cytotoxic activity depends upon multiple factors, including the cytokine microenvironment and interactions with other cells of the immune system, such as macrophages, T cells, and DCs (15). A number of receptors expressed on NK cells participate in their activation by DCs, including NKp30, NKp44, DNAM1, and 2B4 (30, 42). Furthermore, the production of cytokines, such as IL-12, IL-15, and IL-18, by DCs is important for activation and homeostasis of NK cells (42). Like the TCR on T cells, the NK cell receptors form IS with DCs (18). In this study, we demonstrated that the inhibition of Cx43-mediated GJIC between mDCs and NK cells strongly reduced the NK cell activation, as shown by the reduced expression of CD69, CD25, and IFN- $\gamma$  secretion. These data suggest that, like T cells, NK cells require intercellular molecular transport of secondary messengers via GJs from the DCs for their activation, although the nature of these signals remains to be investigated. Cx43-mediated interaction between NK and DCs did not seem to affect DC maturation or TNF- $\alpha$  and IL-12 release. Together, our results indicate that Cx43-mediated GJIC may play a relevant role in regulating the signaling from DCs to NK cells, similar to our previous findings in T cells (14).

NK cell-mediated cytotoxicity is induced by a process involving receptor recognition of ligands on the target cells, followed by IS formation, granule polarization, and release of granular contents into the target cell (20). The formation of the NK cell–target cell synapse is tightly controlled by activating and inhibitory receptors expressed on the NK cells (20). The granular contents include granzymes, which induce apoptosis in the target cell by triggering caspase activity. GrB induces apoptosis by activating caspase-3 and may also induce apoptosis by cleaving Bid and ICAD directly (43). Until recently, the process of NK cells granular content release into the cytosol was unclear. It was

known that perforin was required, but the pores formed by perforin were thought to be too small to allow granzymes to enter the cytosol. However, Thiery et al. (21) have shown that perforin and GrB are endocytosed in a  $\text{Ca}^{2+}$ -dependent manner in large endosomes, which they called gigantesomes, within the target cell near the synapse. The authors proposed that disruption of this gigantesome leads to release of GrB into the cytosol. Whereas Cx43 was found to inhibit NK cell-mediated cytotoxicity of K562 and melanoma cell lines, it did not disrupt degranulation of the target cells. Furthermore, Cx43 significantly inhibited GrB activity and  $\text{Ca}^{2+}$  levels in the target cells. These findings suggest that accumulation of Cx43 at the site of contact between NK and target cells may play a role in gigantesome formation and stabilization and/or contribute to their content release. Further studies will be needed to conclusively demonstrate this hypothesis.

This is the first study, to our knowledge, demonstrating that GJ formation is important for NK cell-mediated lysis. Our data indicate that reduced Cx43 expression might be a valuable mechanism for immune evasion of malignant or pathogen-infected cells. Indeed, it is known that many tumor cells, including colorectal (44) and breast cancer cells (45), downregulate Cx43 expression during epithelial-to-mesenchymal transition. Importantly, the induction of epithelial-to-mesenchymal transition increases tumor resistance to Ag-specific CTL lysis (46, 47), pointing to a possible link between the loss of Cx43 expression and the acquisition of resistance to immune-mediated tumor lysis. Therefore, examining the expression levels of Cx43 in tumors may be an important strategy to design appropriate immune therapeutic treatments.

## Acknowledgments

We thank Prof David Becker for the kind gift of the Cx43 s and AS ODNs and Dr. María Carmen Molina and Dr. Carolina Ribeiro for the kind gift of anti-MICA and MICB Abs.

## Disclosures

The authors have no financial conflicts of interest.

## References

1. Segretain, D., and M. M. Falk. 2004. Regulation of connexin biosynthesis, assembly, gap junction formation, and removal. *Biochim. Biophys. Acta* 1662: 3–21.
2. Harris, A. L. 2007. Connexin channel permeability to cytoplasmic molecules. *Prog. Biophys. Mol. Biol.* 94: 120–143.
3. Söhl, G., and K. Willecke. 2004. Gap junctions and the connexin protein family. *Cardiovasc. Res.* 62: 228–232.
4. Neijssen, J., B. Pang, and J. Neeffjes. 2007. Gap junction-mediated intercellular communication in the immune system. *Prog. Biophys. Mol. Biol.* 94: 207–218.
5. Oviedo-Orta, E., and W. Howard Evans. 2004. Gap junctions and connexin-mediated communication in the immune system. *Biochim. Biophys. Acta* 1662: 102–112.
6. Oviedo-Orta, E., T. Hoy, and W. H. Evans. 2000. Intercellular communication in the immune system: differential expression of connexin40 and 43, and perturbation of gap junction channel functions in peripheral blood and tonsil human lymphocyte subpopulations. *Immunology* 99: 578–590.
7. Oviedo-Orta, E., P. Gasque, and W. H. Evans. 2001. Immunoglobulin and cytokine expression in mixed lymphocyte cultures is reduced by disruption of gap junction intercellular communication. *FASEB J.* 15: 768–774.
8. Zahler, S., A. Hoffmann, T. Gloe, and U. Pohl. 2003. Gap-junctional coupling between neutrophils and endothelial cells: a novel modulator of transendothelial migration. *J. Leukoc. Biol.* 73: 118–126.
9. Neijssen, J., C. Herberths, J. W. Drijfhout, E. Reits, L. Janssen, and J. Neeffjes. 2005. Cross-presentation by intercellular peptide transfer through gap junctions. *Nature* 434: 83–88.
10. Mendoza-Naranjo, A., P. J. Saéz, C. C. Johansson, M. Ramírez, D. Mandakovic, C. Pereda, M. N. López, R. Kiessling, J. C. Sáez, and F. Salazar-Onfray. 2007. Functional gap junctions facilitate melanoma antigen transfer and cross-presentation between human dendritic cells. *J. Immunol.* 178: 6949–6957.
11. Matsue, H., J. Yao, K. Matsue, A. Nagasaka, H. Sugiyama, R. Aoki, M. Kitamura, and S. Shimada. 2006. Gap junction-mediated intercellular communication between dendritic cells (DCs) is required for effective activation of DCs. *J. Immunol.* 176: 181–190.
12. Bopp, T., C. Becker, M. Klein, S. Klein-Hessling, A. Palmetshofer, E. Serfling, V. Heib, M. Becker, J. Kubach, S. Schmitt, et al. 2007. Cyclic adenosine

- monophosphate is a key component of regulatory T cell-mediated suppression. *J. Exp. Med.* 204: 1303–1310.
13. Elgueta, R., J. A. Tobar, K. F. Shoji, J. De Calisto, A. M. Kalergis, M. R. Bono, M. Roseblatt, and J. C. Sáez. 2009. Gap junctions at the dendritic cell-T cell interface are key elements for antigen-dependent T cell activation. *J. Immunol.* 183: 277–284.
  14. Mendoza-Naranjo, A., G. Bouma, C. Pereda, M. Ramírez, K. F. Webb, A. Tittarelli, M. N. López, A. M. Kalergis, A. J. Thrasher, D. L. Becker, and F. Salazar-Onfray. 2011. Functional gap junctions accumulate at the immunological synapse and contribute to T cell activation. *J. Immunol.* 187: 3121–3132.
  15. Vivier, E., E. Tomasello, M. Baratin, T. Walzer, and S. Ugolini. 2008. Functions of natural killer cells. *Nat. Immunol.* 9: 503–510.
  16. Fernandez, N. C., A. Lozier, C. Flament, P. Ricciardi-Castagnoli, D. Bellet, M. Suter, M. Perricaudet, T. Tursz, E. Maraskovsky, and L. Zitvogel. 1999. Dendritic cells directly trigger NK cell functions: cross-talk relevant in innate anti-tumor immune responses in vivo. *Nat. Med.* 5: 405–411.
  17. Woo, C. Y., T. M. Clay, H. K. Lyerly, M. A. Morse, and T. Osada. 2006. Role of natural killer cell function in dendritic cell-based vaccines. *Expert Rev. Vaccines* 5: 55–65.
  18. Barreira da Silva, R. B., and C. Münz. 2011. Natural killer cell activation by dendritic cells: balancing inhibitory and activating signals. *Cell. Mol. Life Sci.* 68: 3505–3518.
  19. Jacobs, B., and E. Ullrich. 2012. The interaction of NK cells and dendritic cells in the tumor environment: how to enforce NK cell & DC action under immunosuppressive conditions? *Curr. Med. Chem.* 19: 1771–1779.
  20. Orange, J. S. 2008. Formation and function of the lytic NK-cell immunological synapse. *Nat. Rev. Immunol.* 8: 713–725.
  21. Thiery, J., D. Keefe, S. Boulant, E. Boucrot, M. Walch, D. Martinvalet, I. S. Goping, R. C. Bleackley, T. Kirchhausen, and J. Lieberman. 2011. Perforin pores in the endosomal membrane trigger the release of endocytosed granzyme B into the cytosol of target cells. *Nat. Immunol.* 12: 770–777.
  22. López, M. N., C. Pereda, G. Segal, L. Muñoz, R. Aguilera, F. E. González, A. Escobar, A. Ginesta, D. Reyes, R. González, et al. 2009. Prolonged survival of dendritic cell-vaccinated melanoma patients correlates with tumor-specific delayed type IV hypersensitivity response and reduction of tumor growth factor  $\beta$ -expressing T cells. *J. Clin. Oncol.* 27: 945–952.
  23. Aguilera, R., C. Saffie, A. Tittarelli, F. E. González, M. Ramírez, D. Reyes, C. Pereda, D. Hevia, T. García, L. Salazar, et al. 2011. Heat-shock induction of tumor-derived danger signals mediates rapid monocyte differentiation into clinically effective dendritic cells. *Clin. Cancer Res.* 17: 2474–2483.
  24. Qiu, C., P. Coutinho, S. Frank, S. Franke, L. Y. Law, P. Martin, C. R. Green, and D. L. Becker. 2003. Targeting connexin43 expression accelerates the rate of wound repair. *Curr. Biol.* 13: 1697–1703.
  25. Dransfield, I., and N. Hogg. 1989. Regulated expression of Mg<sup>2+</sup> binding epitope on leukocyte integrin alpha subunits. *EMBO J.* 8: 3759–3765.
  26. Theorell, J., H. Schlums, S. C. C. Chiang, T. Y. Huang, A. Tattermusch, S. M. Wood, and Y. T. Bryceson. 2011. Sensitive and viable quantification of inside-out signals for LFA-1 activation in human cytotoxic lymphocytes by flow cytometry. *J. Immunol. Methods* 366: 106–118.
  27. Czyz, J., U. Irmer, G. Schulz, A. Mindermann, and D. F. Hülser. 2000. Gap-junctional coupling measured by flow cytometry. *Exp. Cell Res.* 255: 40–46.
  28. Réthi, B., C. Detre, P. Gogolák, A. Kolonics, M. Magócsi, and E. Rajnavölgyi. 2002. Flow cytometry used for the analysis of calcium signaling induced by antigen-specific T-cell activation. *Cytometry* 47: 207–216.
  29. Guan, X., S. Wilson, K. K. Schlender, and R. J. Ruch. 1996. Gap-junction disassembly and connexin 43 dephosphorylation induced by 18  $\beta$ -glycyrrhetic acid. *Mol. Carcinog.* 16: 157–164.
  30. Ferlazzo, G., M. L. Tsang, L. Moretta, G. Melioli, R. M. Steinman, and C. Münz. 2002. Human dendritic cells activate resting natural killer (NK) cells and are recognized via the Nkp30 receptor by activated NK cells. *J. Exp. Med.* 195: 343–351.
  31. Jinushi, M., T. Takehara, T. Kanto, T. Tatsumi, V. Groh, T. Spies, T. Miyagi, T. Suzuki, Y. Sasaki, and N. Hayashi. 2003. Critical role of MHC class I-related chain A and B expression on IFN- $\alpha$ -stimulated dendritic cells in NK cell activation: impairment in chronic hepatitis C virus infection. *J. Immunol.* 170: 1249–1256.
  32. Decrock, E., M. Vinken, E. De Vuyst, D. V. Krysko, K. D'Herde, T. Vanhaecke, P. Vandenabeele, V. Rogiers, and L. Leybaert. 2009. Connexin-related signaling in cell death: to live or let die? *Cell Death Differ.* 16: 524–536.
  33. Voskoboinik, I., M. J. Smyth, and J. A. Trapani. 2006. Perforin-mediated target-cell death and immune homeostasis. *Nat. Rev. Immunol.* 6: 940–952.
  34. Smyth, M. J., S. E. Street, and J. A. Trapani. 2003. Cutting edge: granzymes A and B are not essential for perforin-mediated tumor rejection. *J. Immunol.* 171: 515–518.
  35. Kim, M., C. V. Carman, and T. A. Springer. 2003. Bidirectional transmembrane signaling by cytoplasmic domain separation in integrins. *Science* 301: 1720–1725.
  36. Bryceson, Y. T., M. E. March, D. F. Barber, H. G. Ljunggren, and E. O. Long. 2005. Cytolytic granule polarization and degranulation controlled by different receptors in resting NK cells. *J. Exp. Med.* 202: 1001–1012.
  37. Krzewski, K., A. Gil-Krzewska, V. Nguyen, G. Peruzzi, and J. E. Coligan. 2013. LAMP1/CD107a is required for efficient perforin delivery to lytic granules and NK-cell cytotoxicity. *Blood* 121: 4672–4683.
  38. Maul-Pavicic, A., S. C. Chiang, A. Rensing-Ehl, B. Jessen, C. Fauriat, S. M. Wood, S. Sjöqvist, M. Hufnagel, I. Schulze, T. Bass, et al. 2011. ORAI1-mediated calcium influx is required for human cytotoxic lymphocyte degranulation and target cell lysis. *Proc. Natl. Acad. Sci. USA* 108: 3324–3329.
  39. Cotrina, M. L., J. H. Lin, A. Alves-Rodrigues, S. Liu, J. Li, H. Azmi-Ghadimi, J. Kang, C. C. Naus, and M. Nedergaard. 1998. Connexins regulate calcium signaling by controlling ATP release. *Proc. Natl. Acad. Sci. USA* 95: 15735–15740.
  40. Lopez, J. A., M. R. Jenkins, J. A. Rudd-Schmidt, A. J. Brennan, J. C. Danne, S. I. Manning, J. A. Trapani, and I. Voskoboinik. 2013. Rapid and unidirectional perforin pore delivery at the cytotoxic immune synapse. *J. Immunol.* 191: 2328–2334.
  41. Decrock, E., M. Vinken, M. Bol, K. D'Herde, V. Rogiers, P. Vandenabeele, D. V. Krysko, G. Bultynck, and L. Leybaert. 2011. Calcium and connexin-based intercellular communication, a deadly catch? *Cell Calcium* 50: 310–321.
  42. Vivier, E., D. H. Raulet, A. Moretta, M. A. Caligiuri, L. Zitvogel, L. L. Lanier, W. M. Yokoyama, and S. Ugolini. 2011. Innate or adaptive immunity? The example of natural killer cells. *Science* 331: 44–49.
  43. Cullen, S. P., C. Adrain, A. U. Lüthi, P. J. Duriez, and S. J. Martin. 2007. Human and murine granzyme B exhibit divergent substrate preferences. *J. Cell Biol.* 176: 435–444.
  44. Lee, C. C., W. S. Chen, C. C. Chen, L. L. Chen, Y. S. Lin, C. S. Fan, and T. S. Huang. 2012. TCF12 protein functions as transcriptional repressor of E-cadherin, and its overexpression is correlated with metastasis of colorectal cancer. *J. Biol. Chem.* 287: 2798–2809.
  45. McLachlan, E., Q. Shao, H. L. Wang, S. Langlois, and D. W. Laird. 2006. Connexins act as tumor suppressors in three-dimensional mammary cell organoids by regulating differentiation and angiogenesis. *Cancer Res.* 66: 9886–9894.
  46. Kudo-Saito, C., H. Shirako, T. Takeuchi, and Y. Kawakami. 2009. Cancer metastasis is accelerated through immunosuppression during Snail-induced EMT of cancer cells. *Cancer Cell* 15: 195–206.
  47. Akalay, I., B. Janji, M. Hasmim, M. Z. Noman, F. André, P. De Cremoux, P. Bertheau, C. Badoual, P. Vielh, A. K. Larsen, et al. 2013. Epithelial-to-mesenchymal transition and autophagy induction in breast carcinoma promote escape from T-cell-mediated lysis. *Cancer Res.* 73: 2418–2427.